HIGH-FIELD FLUX PINNING AND THE STRAIN SCALING LAW*

J. W. Ekin
Electromagnetic Technology Division
National Bureau of Standards
Boulder, Colorado 80303

The effects of strain on flux pinning in superconductors are discussed. Significant differences between the strain scaling law, temperature scaling law, and the flux-line-shearing model of Kramer are demonstrated. The strain scaling law is more general than current flux-pinning models, and as such, it may serve as a guide to future work on flux pinning theory. Flux-pinning measurements at fields up to 24 T have been made on a series of high-quality Nb_3Sn samples with third (and fourth) element additions. The data show that the usual extrapolation procedures for determining the bulk-average upper critical field in Nb_3Sn lead to significant errors when additives such as Ti, Ta, Ga, and Hf are present.

INTRODUCTION

The effects of strain on flux pinning in superconductors were observed to obey scaling behavior in 1980 and systematized into what is called the strain scaling law (SSL) [1]. The practical significance of SSL is two fold. First, as will be shown, it is more general than current theories of flux pinning and as such, it serves as a guide to future work on flux pinning theory. It is different from the temperature scaling law (TSL) of Fietz and Webb [2] and cannot be derived from Kramer's flux-line-shearing model [3]. Second, it can be used to calculate the peak (strain-free) critical-current density (J_c) in practical superconductors from measurements of J_c obtained on the conductor in its initial strained state.

This paper describes the differences between the SSL, the TSL, and the flux-line-shearing model in an effort to clarify the successes and deficiencies of our current understanding of flux pinning. The paper also shows that the usual extrapolation procedures for determining the bulk upper critical field in Nb_3Sn conductors with additives can lead to large errors in determining this practical parameter. The technique for using the SSL to correct J_c measurements on practical conductors will be presented in detail elsewhere.

STRAIN SCALING LAW

The strain scaling law (SSL) describes the strain dependence of the pinning force ($F \equiv J_c B$). Basically, it states that the shape of the curve of the pinning force as a function of reduced magnetic field is not changed by the application of strain to a superconductor. If we let b represent the reduced magnetic field $b \equiv B/B^*_{c2}$ (where the star implies a bulk-average upper-critical field $B^*_{c2} \equiv \mu_o H^*_{c2}$, described in more detail below) and if we let f(b) represent the shape of the pinning force curve, then the SSL may be expressed as:

$$F = [B^*_{c2}(\varepsilon)]^v f(b) \qquad (1)$$

In Eq. (1), the proportionality constant between F and f(b) is independent of field, but varies with strain as $[B^*_{c2}(\varepsilon)]^v$, where v is a constant independent of both field and strain. The value of v changes for different superconductor compounds, but has been empirically determined to be essentially the same for all types of conductors of the same compound.[1] For example, v = 1 for all types of Nb_3Sn conductors, including conductors made by "bronze-process", "in-situ", "jelly-roll", internal-tin, and liquid-tin-infiltration techniques.

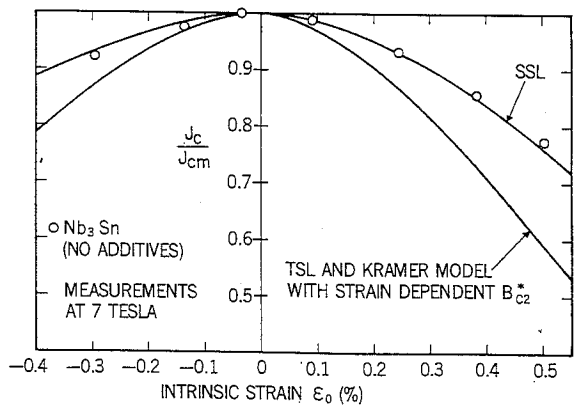

Fig. 1. Comparison between J_c-strain data and the results of the strain scaling law (SSL) [1], temperature scaling law (TSL) [2], and flux-line-shearing model of Kramer [3]. Data are for the strand material used in the Nb_3Sn LCP coil.

DIFFERENCES BETWEEN THE SSL, TSL, AND KRAMER THEORY

The SSL described in Eq. (1) is different from the temperature scaling law (TSL) observed by Fietz and Webb [2]. The TSL describes the effect of temperature on the pinning force in superconductors. Using the same terminology as in Eq. (1), the TSL may be written:

$$F = [B_{c2}(T)]^{2.5} f(b) \qquad (2)$$

where $b \equiv B/B_{c2}(T)$ and the proportionality constant between F and f(b) has a temperature dependence proportional to $[B_{c2}(T)]^{2.5}$. Note the difference between the two scaling laws. The power of the prefactor for strain scaling is about 1 for Nb_3Sn, not 2.5 as for temperature scaling.

Following the observation of temperature scaling, a flux-line-shearing model for flux pinning in superconductors was developed by Kramer [3] to explain Eq. (2). The model has met with considerable success in Nb_3Sn, but not in other superconductors (see below). The flux pinning model of Kramer is often confused with the empirical temperature scaling law of Fietz and Webb, and is even sometimes referred to as the Kramer Scaling Law. Actually this is a misnomer. The flux pinning theory of Kramer postdates the temperature scaling law of Fietz and Webb by four years and is more restrictive, applying principally to Nb_3Sn.

The strain scaling law cannot be obtained from either the TSL or the Kramer model, even for the case of binary Nb_3Sn. The model developed by Kramer to explain the TSL states that:

$$F = C_s \kappa_1^{-2} (B^*_{c2})^{2.5} b^{0.5} (1-b)^2 \qquad (3)$$

where κ_1 is the Ginzburg-Landau parameter and C_s is a number that depends on the density of strong line pins. No consideration is given to strain in the TSL and Kramer model. Furthermore, if the temperature-dependent $B_{c2}(T)$ is simply replaced by a strain-dependent $B^*_{c2}(\varepsilon)$, as has been tried in the past [4], the resulting expression does not agree with the data. An example is shown in Fig. 1. Data obtained on a practical Nb_3Sn conductor are shown by open circles. The lower solid curve is obtained when values of the strain-dependent $B^*_{c2}(\varepsilon)$ measured on this conductor are substituted into the TSL and Kramer model expressions, Eqs. (2) and (3). The upper solid curve, on the other hand, is obtained from the SSL, Eq. (1). The discrepancy between the data and the results of the TSL and Kramer model expressions is significant; the discrepancies are even greater for materials other than binary Nb_3Sn. On the other hand, the results of the SSL agree quite well with the data.

The SSL has been observed to show agreement similar to that in Fig. 1 for many materials other than Nb_3Sn where the Kramer model clearly does not apply, such as V_3Ga [5], NbTi [6], or Nb_3Sn-with-additives (see discussion below). In these materials, the field dependence of the pinning force f(b) is significantly different from that given in Eq. (3). An example of strain scaling in such a material is shown for V_3Ga in Figs. 2a and 2b. Note in Figs. 2 that the flux pinning force approaches zero linearly as (1-b), not quadratically as $(1-b)^2$ given by the Kramer model. Yet the data show precise strain scaling over a wide range of uniaxial strain and magnetic field (i.e. the shape of the flux pinning curve with applied strain is invariant).

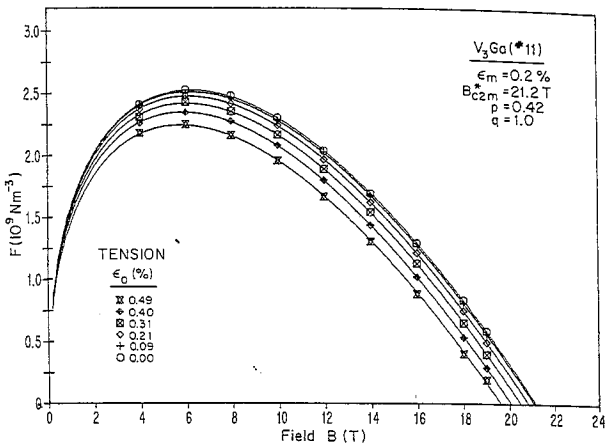

Fig. 2a. Pinning-force density F vs. magnetic field at different intrinsic tensile strains ε_o in V_3Ga. Curves are drawn using Eq. (4) and the values of p and q shown in the figure.

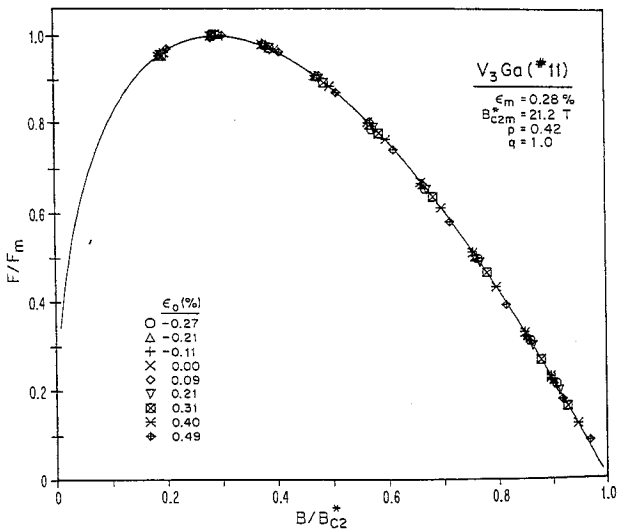

Fig. 2b. Normalized plot of the data in Fig. 2a, demonstrating strain scaling in a superconductor that does not fit the flux-line-shearing-model expression, Eq. (3). F has been normalized by its strain-dependent maximum value F_m, and the field has been normalized by the strain-dependent bulk-average upper critical field B^*_{c2}.

Information on flux pinning can also be obtained from the details of the strain-scaling parameters in each of these materials, when compared with Nb_3Sn. In materials such as Nb_3Sn-with-additives or V_3Si, the SSL has exactly the same form as for binary Nb_3Sn. In V_3Ga, the power of the prefactor, v, is enhanced slightly, with v = 1.4. In NbTi where the pinning mechanism is not the same as in compound superconductors, the value of v is considerably higher than 1. However, in all these superconductors, the power of the prefactor for strain scaling is significantly different from that for temperature scaling in the same material. Also the value of v in the strain scaling law does not change for different types of conductors of the same material (e.g. bronze process, in-situ, powder metallurgy, etc.).

Thus, the scaling of the pinning force with strain is a very general law, applicable to many superconductors for which the Kramer model does not apply. It is also significantly different from the TSL and Kramer model, and as such, it may serve as a guide for future work on flux-pinning theory.

For example, the SSL suggests that there are terms in the prefactor of the flux pinning model expression other than B_{c2} which depend on strain. This is necessary in order to account for both the temperature and strain scaling laws with the same model expression. Such a strain dependence may arise from strain being concentrated locally at the grain boundaries, increasing the strength or spatial extent of the grain-boundary pinning interaction. The presence of such a term that increases with strain could compensate the decrease in the B_{c2} term in the prefactor and account for the smaller power law of the prefactor in the SSL compared with the TSL. Strain dependence could also enter through κ.

Another point to consider when modeling the pinning interaction is the similarity of the strain scaling law in V_3Ga and Nb_3Sn. Apparently the terms in the prefactor do not change drastically between these two materials although the form of f(b) is significantly different, $(1-b)$ compared to $(1-b)^2$.

SHAPE OF HIGH-FIELD PINNING CURVE IN Nb_3Sn WITH ADDITIVES

We now turn from the subject of the differences between the strain and temperature scaling laws and focus on the details of the shape of the flux-pinning-versus-field curve, f(b), in Nb_3Sn. The following discussion applies equally to both the SSL and the TSL. Specifically, it is shown that even Nb_3Sn does not conform to the Kramer expression for f(b) when additives are present.

Pinning theories suggest that f(b) has the general form:

$$f(b) = C\, b^p (1-b)^q \qquad (4)$$

where C is a proportionality constant and $b \equiv B/B_{c2}$. For binary Nb_3Sn, p = 0.5 and q = 2.0, which are the values given by Kramer's flux-line shearing model, Eq (3).

However, the addition of third (and fourth) elements to Nb_3Sn tends to linearize the shape of the f(b) curve at high fields, reducing the value of q from 2 towards unity. This was first shown several years ago when q was reported to be reduced to about 1.1 in Nb_3Sn samples with Hf and Ga additions.[7]

Table I. Strain Scaling Parameters for Nb_3Sn with Various Additives (in at%)

$$F = C[B^*_{c2}(\varepsilon)]^v\, [B/B^*_{c2}(\varepsilon)]^p\, \{1 - [B/B^*_{c2}(\varepsilon)]\}^q$$

	Shape of $J_c(B)$		Bulk-average Upper-critical Field (T)	Strain Sensitivity of B^*_{c2}: $d \ln(B^*_{c2})/d(\lvert\varepsilon\rvert^{1.7})$		Strain Sensitivity of F_{max}
	p	q	B^*_{c2m}	(ε_o<0)	(ε_o>0)	v
Nb_3Sn	0.5	2.0	21	900	1250	1.0
Nb-5Hf/Cn-5Sn-4Ga	0.4	1.1	25	900	1250	1.1
Nb_3Sn+0.6Ti	0.6	1.7	23	900	1250	1.1
Nb_3Sn+1.85Ti	0.5	1.5	25	1100	1450	1.2
Nb_3Sn+0.6Ta	0.5	1.4	24	900	1250	1.0
Nb_3Sn+2.2Ta	0.5	1.7	25	1400	1800	1
Nb_3Sn+0.2H	0.7	2.2	25	1400	1800	---

Here we report a similar reduction in q to less than 2 for essentially all other practical additives to Nb_3Sn, including Ti, Ta, Ga, and Hf. The results are summarized in Table I. As seen in Table I, values of q are reduced typically to the range 1 to 1.7 depending on the additive, its concentration (and possibly the heat treatment conditions). [8]

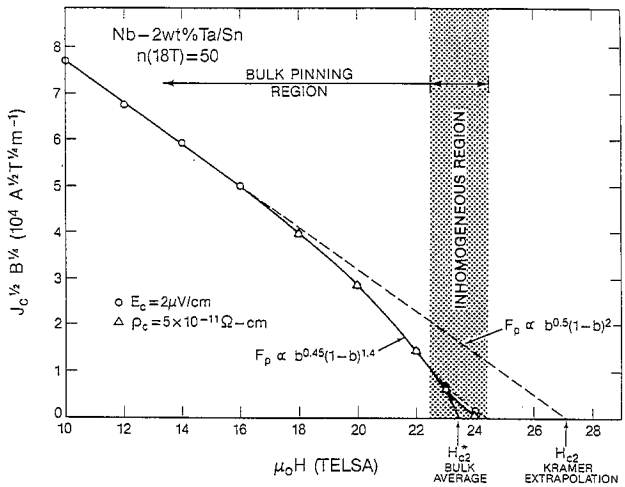

Fig. 3. Deviation of the high-field flux pinning curve from the Kramer model expression in a high-quality (high-n) Nb_3Sn sample with Ta additions. A straight line extrapolation on this type of plot overvalues B^*_{c2} in this conductor by about 4 T. A fit to the general pinning expression in Eq. (4) yields a $(1-b)^{1.4}$ high-field dependence and a B^*_{c2} of 23.4 T.

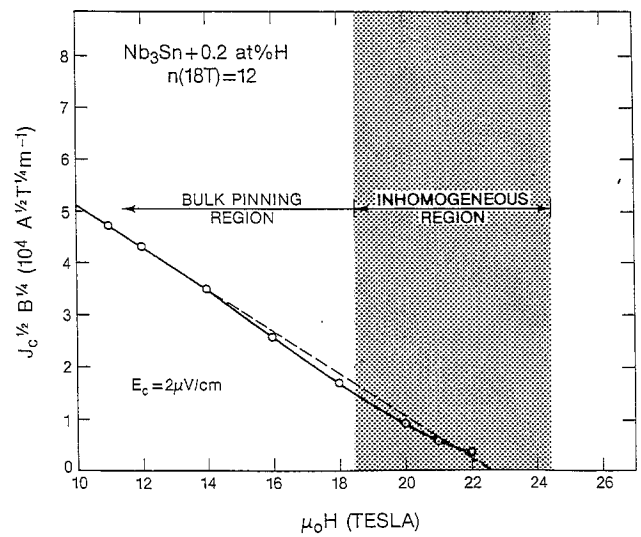

Fig. 4. Masking of the high-field flux-pinning curve by a wide range of B_{c2} due to material inhomogeneity in a low-n Nb_3Sn sample with hydrogen additions.

An example of this reduction of q below 2 is shown for Ta additions in Fig. 3. The J_c data have been replotted in the usual manner using a Kramer plot to illustrate their deviation from the high-field q = 2 dependence given in Eq. (3). Such a dependence would be a straight line on this type of plot and is shown by the dashed line in Fig. 3. This type of plot is used for illustration purposes only; in general, a simple pinning force vs. B plot is preferred, as discussed below. Notice in Fig. 3 that at fields above about 18 T the data deviate below a straight-line (q = 2) dependence. A least-squares fit to f(b) in terms of p, q, B^*_{c2}, and a proportionality constant, results in q = 1.4 (p = 0.45 and B^*_{c2} = 23.4 T). Thus, the effect of the additive results not only in an increase in B^*_{c2}, but also a decrease in q below the binary-Nb_3Sn value of 2.

The decrease in q in Fig. 3 is independent of the criterion used to determine J_c. For this sample, the quality factor "n" (describing the sharpness of the take-off of the V-I curve [9]) had a value of 50 at 18 T, indicating a relatively homogeneous sample. This value of n is very high compared with most Nb_3Sn samples at 18 T. As shown in Fig. 3, a re-analysis of the data in terms of a resistivity criterion instead of an electric-field criterion resulted in the same shaped curve, except very near B^*_{c2}.

EFFECT OF INHOMOGENEITY OF B_{c2} ON THE SHAPE OF HIGH-FIELD PINNING CURVES

Referring again to Table I, note that the last sample containing H additions was the only sample we have measured which did not have a q value lower than 2. This sample, however, makes an interesting point regarding how local inhomogeneity of B_{c2} within the superconducting material can mask the intrinsic shape of the flux-pinning curve at high fields.

Figure 4 shows a Kramer plot of the data for this sample. Note that the value of n for this sample was quite low, only 12 at 18 T (compared with a value of 50 at 18 T for the sample containing Ta additions shown in Fig. 3). This low value of n is suggestive of a wide range of B_{c2} due to sample inhomogeneity.

If such a range of B_{c2} due to sample inhomogeneity exists, it would cause a tailing effect, or region of positive curvature in the pinning curve (over the field range where portions of the sample with the lowest values of B_{c2} progressively become normal). This tail can mask the true shape of the f(b) curve and, if extensive enough, can cause a wide region of positive curvature (q > 2) as is evident starting at about 18 T in Fig. 4. As a result, the value of q will appear much higher than its intrinsic value in samples with a wide range of B_{c2}.

The region where this tailing effect starts to become significant in Fig. 4 (i.e., where the curve changes from negative curvature to positive curvature) is shaded and indicated as the range of B_{c2} due to inhomogeneity that could cause such a tail. For comparison, the relatively narrow range of B_{c2} that could cause the small tail for the Ta-additive sample is also shown as a shaded region in Fig. 3.

Because of the low n and the suspected wide range of B_{c2} in the sample with H additions, it is quite possible that even this sample has a significantly reduced q compared with binary Nb_3Sn, similar to the other Nb_3Sn-with-additive samples in Table I. The start of such a decrease below the q = 2 line in Fig. 4 can be seen in the range between 14 and 18 T before the tailing effect starts. Thus, care should be exercised in drawing conclusions about intrinsic high-field pinning characteristics from inhomogeneous samples.

EXTRAPOLATION PROCEDURES FOR OBTAINING B^*_{c2}

The deviation of the shape of f(b) from the Kramer model described in the previous section has several practical consequences for determining the bulk-average upper critical field B^*_{c2}. B^*_{c2} is a significant, practical parameter. The SSL can be used with inhomogeneous superconductors (and most practical superconductors are inevitably inhomogeneous to some degree) only if the bulk-average B^*_{c2} is used.[1] Scaling does not work if the upper limit of the B_{c2} range is used, i.e. the value of field where the last remnant of superconductivity disappears, usually determined inductively or resistively.[1,10] The bulk-average B^*_{c2} also serves as a practical figure of merit in evaluating candidate superconductors for magnet applications.

The usual practice to determine the bulk average B^*_{c2} for Nb_3Sn is to use a straight-line extrapolation on a plot such as that in Figs. 3 or 4. However, this can lead to significant errors. In Nb_3Sn conductors with Ti or Ta additions, B^*_{c2} is typically overvalued by about 3-5 T, as seen in Fig. 3. A much more accurate procedure is to make extrapolations by fitting the shape of f(b) to a general pinning function such as that in Eq. (4) in terms of the four parameters B^*_{c2}, p, q, and C. An equal-weight least-squares fit of this function to the pinning-force vs. B characteristic (such as shown in Figs. 2) de-emphasizes the tailing region and has proven useful in determining intrinsic bulk-average values of B^*_{c2}.

CONCLUSIONS

1. The strain scaling law is different from the temperature scaling law. For example, the power of the prefactor for strain scaling is about 1 rather than 2.5 for Nb_3Sn.

2. Strain effect data fit the strain scaling law in superconductors like V_3Ga, NbTi, or Nb_3Sn-with-additives, where the flux-line-shearing model of Kramer does not apply. Thus, the scaling of the pinning force with strain is a very general law, more universal than the current theories of flux pinning. There is a need to incorporate strain as a parameter into present fluxpinning theory and explain the consistent scaling behavior represented by the SSL.

3. Additions of third (and fourth) elements such as Ti, Ta, Ga, and Hf to binary Nb_3Sn tend to linearize the shape of the f(b) curve at high fields, causing significant deviations from the Kramer-model expression, Eq. (3). As a result of this deviation, the usual practice of determining the bulk-average B^*_{c2} using a Kramer-type plot such as Fig. 3 leads to a significant overvaluation of B^*_{c2}, typically 3 to 5 T. A much more accurate procedure is to determine B^*_{c2} by a least-squares fit of J_c data (away from the inhomogeneous region) to a general pinning function such as that in Eq. (4).

4. A range of upper critical fields due to sample inhomogeneity can lead to a tailing effect which masks the intrinsic shape of the flux pinning curve at high fields. Such inhomogeneity, if extensive enough, can lead to artificially high values of q which are unrepresentative of the bulk material.

ACKNOWLEDGEMENTS

The assistance of J. Brauch, D. Rule, and V. Cima in analyzing these data is gratefully acknowledged. Helpful discussions were held with L. F. Goodrich, A. F. Clark, R. B. Goldfarb, D. Welch, M. Suenaga, and D. Larbalestier. This work was sponsored by the Department of Energy, Office of Fusion Energy under inter-agency agreement #DE-AI01-84ER52113. The high magnetic fields needed for this study were obtained using the magnet facilities of the Francis Bitter National Magnet Laboratory.

REFERENCES

1) J. W. Ekin, Cryogenics 20, 614 (1980).
2) W. A. Fietz and W. W. Webb, Phys. Rev. 178, 657 (1969).
3) E. J. Kramer, J. Appl. Phys. 44, 1360 (1973).
4) See, for example, G. Rupp, IEEE Trans. Mag. MAG-15, 189 (1979).
5) See, for example, J. W. Ekin, IEEE Trans. Mag. MAG-17, 658 (1981).
6) See, for example, D. C. Larbalestier, IEEE Trans. Mag. MAG-17, 1668 (1981).
7) J. W. Ekin, H. Sekine, and K. Tachikawa, J. Appl. Phys. 52, 6252 (1981).
8) See also paper A7 in these conference proceedings by D. O. Welch, M. Suenaga, C. L. Snead, Jr., and R. D. Hatcher.
9) See, for examples, F. Voelker, Particle Accelerators 1, 205 (1970); J. W. Ekin, J. Appl. Phys. 49, 3406 (1978); L. F. Goodrich and F. R. Fickett, Cryogenics 22, 225 (1982).
10) D. M. Kroeger, D. S. Easton, A. DasGupta, C. C. Koch, and J. O. Scarbrough, J.